From Piecewise-Linear to Piecewise-Circular: A Geometric Extension of Integration Theory via Osculating Sectors

Abstract
This paper introduces the D'Ambrosio Integral, a geometrically oriented generalization of the Riemann integral that incorporates the curvature of the integrable curve. Unlike classical schemes based on linear approximation, the proposed method employs circular arcs determined by consecutive triplets of points, allowing curvature information to be directly embedded into the integration process. It is shown that the integral converges, is geometrically invariant, and coincides with the Riemann integral for sufficiently smooth functions. The formulation naturally extends to Riemannian manifolds through the use of the exponential map. The proposed approach provides higher geometric accuracy in regions of pronounced curvature and is applicable to the analysis of curves, vector fields, and dynamical systems.

Keywords: Riemann Integral, Geometric integration, Curvature-sensitive Integration, Curvature-based Integration, Geometric modeling, Non-Euclidean geometry, Curves areas, Curves length

UDC 517.5 : 514.18

Authors details

Mr. Giuseppe D'Ambrosio, Senior IT Developer, remote freelancer, damgiu1978@gmail.com, 7, Spadarella, Altavilla Silentina 84045 – Salerno (Italy) (no academic affiliation), +393398089353

1. Introduction

The integral has long served as the fundamental construct for measuring area, length, and volume in mathematical analysis. Historically, all major frameworks, from Riemann's foundational approach to subsequent developments like the Lebesgue and Henstock–Kurzweil integrals (Rudin, 1976; Royden, 1988), have shared a single conceptual limitation: they rely on partitioning a domain and aggregating geometric measures (area, length) via linear segments or simple planar primitives. This inherently restricts the measure to a first-order (polygonal) approximation of the underlying function or curve geometry.

This paper introduces a novel approach that fundamentally supersedes the linear paradigm, establishing a new, curvature-sensitive framework for integration. This method, termed the D'Ambrosio Integral, is rooted in the geometric intuition that any sufficiently regular curve can be locally approximated and ultimately decomposed—not merely by infinitesimal linear segments—but by infinitesimal circular arcs. This insight utilizes the elementary principle that any three non-aligned points uniquely define a circle, allowing the construction to utilize local curvature at every step.

In this new perspective, a curve is conceived as inherently possessing its own local geometric measure, defining an area element derived from its own curvature without reliance on external bounding axes. Our construction replaces the traditional reliance on linear interpolation with circular interpolation defined by consecutive triplets of points along the curve.

This methodology introduces two primary geometric functionals: one for Arc-Based Curve Length, which measures length by summing the segments of these circular arcs, and one for Sector-Based Curvature Area, which measures area by summing the area of the corresponding circular sectors.

The D'Ambrosio Integral fundamentally surpasses the logic of the Riemann paradigm by elevating the approximation order and geometric accuracy. The Riemann integral relies on adding the area of rectangles or trapezoids, which constitutes only a first-order (linear) approximation of the local geometry. The D'Ambrosio Integral, conversely, is built upon the area associated with a partition step by summing the area of the circular arc's sector plus the area of the trapezoid defined by the circular arc, the x-axis, and the vertical lines dropped from the arc's endpoints. In essence, this method is a geometrically elegant variant of the trapezoidal rule that uses circular arcs instead of straight segments. This inclusion of the circular arc's geometry—which matches the curve up to the second derivative (curvature)—makes the approximation locally much more accurate in regions of high curvature. This superior method captures the discrete and determined totality of the curve's geometric measure in the limit, distinguishing it conceptually from a mere polygonal approximation. Furthermore, the classical integral is confined to Euclidean space, whereas the D'Ambrosio construction is intrinsically defined for curves on Riemannian manifolds through the exponential map, immediately extending its utility to non-Euclidean geometries (Do Carmo, 1992).

The resulting integral is well-defined for continuous and sufficiently smooth functions. It provides a robust, curvature-aware framework applicable to smooth vector fields and parameter-dependent dynamical systems, where the resulting functional acts as a powerful invariant quantifying the accumulated geometric sweep of flow trajectories. These capabilities confirm that the D'Ambrosio integral represents a genuinely geometric extension of integration theory, moving beyond the limitations of piecewise-linear measurement.

2. Conceptual review

2.1. Classical Integration frameworks

The foundation of modern integration theory was laid with the introduction of the Riemann integral in the 19th century. This integral approaches the problem of integrating a function by partitioning the domain into intervals and summing the values of the function over these partitions. The method is straightforward and intuitive, yet it has notable limitations, particularly when dealing with functions that exhibit significant discontinuities or unbounded variation. For example, functions with oscillations or discontinuities, such as the Dirichlet function, cannot be properly integrated in the Riemann sense.

To address these limitations, the Lebesgue integral was developed by Henri Léon Lebesgue in the early 20th century. Rather than focusing on partitioning the domain into intervals, the Lebesgue integral measures the range of the function values, integrating with respect to the measure of the sets on which those values occur. This shift in focus from domain intervals to function values allows for the integration of a much broader class of functions, especially those with complex discontinuities. The Lebesgue integral provides a more flexible and powerful tool, especially for handling limits of functions and sequences of functions that exhibit irregular behavior.

However, even the Lebesgue integral has limitations in certain contexts, particularly when dealing with highly irregular functions or applications requiring finer control over the integrals' geometric aspects. To overcome such challenges, several generalizations of the Riemann and Lebesgue integrals have been proposed:

- Henstock–Kurzweil Integral - Also known as the generalized Riemann or gauge integral, the Henstock–Kurzweil Integral extends the Riemann integral by allowing variable partition sizes controlled by a gauge function. This integral can handle functions that are not integrable in the Lebesgue sense, including all derivatives of functions, even those that are not continuous (Henstock, 1955). By providing a more flexible method for partitioning the domain, the

Henstock–Kurzweil Integral allows for the integration of a larger class of functions, especially those that involve irregular or oscillatory behavior.

- McShane Integral - The McShane Integral modifies the Riemann approach by using finer partitions and is equivalent to the Lebesgue integral for bounded functions. This version simplifies the integration process, focusing on the partitioning of the function's domain without heavily relying on the measure theory that underpins the Lebesgue integral. McShane's approach provides a more computationally accessible method for certain types of functions while maintaining the precision of the Lebesgue framework for bounded functions (McShane, 1953).

While each of these integrals broadens the scope of integrable functions, they all maintain a foundational reliance on linear approximations, and thus, their geometric interpretation remains limited.

2.2. Geometric considerations in integration

Classical integration methods, such as the Riemann integral, rely on linear approximations—typically using straight line segments to estimate the area under a curve (Riemann, 1867). While effective for smooth, nearly linear functions, this approach loses accuracy when curvature becomes significant. In these cases, linear segments fail to reflect the actual shape of the curve, leading to poor approximations, especially in applications involving detailed geometry (Press et al., 2007).

Geometric integration techniques, informed by differential geometry, aim to capture the local geometric structure of the function. A central concept is the *osculating circle*, which approximates a curve at a point using a circle matching both its tangent and curvature (first and second derivatives) (Do Carmo, 2016). This approach provides a better local fit than linear methods and is particularly useful in regions of high curvature.

Replacing linear elements with osculating circles improves the fidelity of the approximation, particularly for non-linear functions. This concept underpins the D'Ambrosio Integral, which incorporates curvature explicitly in the integration process. While not yet common in standard integration theory, this idea is conceptually aligned with structure-preserving numerical methods used in geometric integration, where capturing the geometry of a system improves both accuracy and long-term stability (Hairer et al., 2006).

2.3. Limitations of existing integration theories

Most existing integration theories continue to rely on piecewise linear approximations, including Riemann and Lebesgue integrals (Bartle, 2014). This linear framework fails to capture essential geometric features of functions with non-trivial curvature. In domains such as computer graphics, computational geometry, and physics-based modeling, such limitations lead to significant discrepancies between the mathematical model and the real geometry (Botsch et al., 2010).

The D’Ambrosio Integral addresses this gap by replacing linear partitions with circular arcs—geometric primitives that inherently account for curvature. This transition from a linear to a curvature-aware model allows the integral to adapt to the intrinsic geometry of the function. Similar ideas have been explored in geometric integration schemes for dynamical systems, where preserving geometric structure improves long-term accuracy and stability (Hairer et al., 2006).

By embedding curvature directly into the integration process, the D’Ambrosio Integral offers a more robust and faithful approach for integrating non-linear or curved functions.

2.4. Intrinsic and differential perspectives in geometric integration

While curvature-aware methods improve local fidelity, an equally important challenge lies in defining integration in a way that is intrinsic—that is, independent of the coordinate system or embedding space. Differential geometry provides the formal framework for such intrinsic constructions through the exponential map, which connects tangent spaces to manifolds (Do Carmo,

1992). Within this setting, integration can be reinterpreted as a process that accumulates oriented geometric quantities along curves or flow lines on manifolds.

Recent developments in geometric integration and structure-preserving numerical analysis (Hairer et al., 2006; Crane et al., 2013) demonstrate that respecting intrinsic curvature leads to improved stability and accuracy in dynamical systems. The D'Ambrosio Integral builds on these principles by generalizing curvature-sensitive integration from Euclidean curves to Riemannian manifolds, extending its scope to vector fields and differential flows where the integral defines a curvature-dependent invariant.

3. Preliminaries

We begin by introducing the necessary concepts and notations from differential geometry and classical analysis that will serve as the foundation for our construction. Our discussion will primarily concern smooth planar curves in $\mathbb{R}^2$, for which curvature and osculating circles are well defined.

3.1. Regular planar curves

Let $\gamma : I \subset \mathbb{R} \to \mathbb{R}^2$ be a curve of class C^2. We say that γ is regular if $\gamma'(t) \neq 0$ for all $t \in I$. The unit tangent vector $T(t)$ is defined as

$$T(t) = \gamma'(t) / \|\gamma'(t)\|.$$

The curvature $\kappa(t)$ of γ at t is given by

$$\kappa(t) = \|T'(t)\| / \|\gamma'(t)\| = \|\gamma'(t) \times \gamma''(t)\| / \|\gamma'(t)\|^3,$$

where $\times$ denotes the scalar (2D) cross product. For regular curves, $\kappa(t)$ is well-defined and continuous on I.

3.2. The osculating circle

Given a point $\gamma(t_0)$ on a regular curve γ, the osculating circle at t_0 is the unique circle that has the same position, tangent, and curvature as the curve at $\gamma(t_0)$. Its radius is given by $\rho(t_0) = 1 / |\kappa(t_0)|$, and its center lies along the normal vector $N(t_0)$, at a distance $\rho(t_0)$ from $\gamma(t_0)$. The osculating circle provides the second-order best approximation to the curve at a given point and plays a fundamental role in our arc-based decomposition.

3.3. Circle through three points

The following classical result is central to our construction:

Let $A, B, C \in \mathbb{R}^2$ be three non-collinear points. Then there exists a unique circle passing through A, B, and C.

This result follows directly from elementary Euclidean geometry: the perpendicular bisectors of the segments AB and BC intersect at the unique center of the circle, and the radius is given by the distance to any of the three points. For collinear points, the circle is undefined or degenerates to a straight line.

We will exploit this property to generate local interpolating arcs along a given curve, using moving windows of three points sampled from the domain.

3.4. Classical Riemann integral

Given a function $f : [a, b] \to \mathbb{R}$, the Riemann integral is defined via partitions $P = \{x_0, x_1, \ldots, x\_n\}$ of $[a, b]$, with mesh $|P| = \max(x_{i+1} - x_i)$, and the limit

$$\int_a^b f(x)\,dx = \lim\_{|P|\to 0} \sum\_{i=0}^{n-1} f(\xi_i)(x_{i+1} - x_i),$$

where $\xi_i \in [x_i, x_{i+1}]$. Each term represents the area of a rectangle or, geometrically, a straight-line approximation under the graph of *f*.

In the forthcoming section, we propose a modification of this scheme wherein instead of straight-line segments, we interpolate the curve with circular arcs passing through triplets of points $(x_{i-1}, f(x_{i-1}))$, $(x_i, f(x_i))$, and $(x_{i+1}, f(x_{i+1}))$, thereby constructing an arc-based summation scheme.

4. Theoretical framework and intrinsic construction

Let (M, g) be an oriented C^∞ Riemannian manifold of dimension $n \geq 2$. Let $\gamma: [a, b] \to M$ be a C^3 immersed curve. We will work in a compact tubular neighborhood of $\gamma([a, b])$ where the injectivity radius is bounded below by $r_{min} > 0$ and all curvature tensors and covariant derivatives up to the order required are uniformly bounded.

4.1. Exponential circle and oriented sector (intrinsic)

Fix $t \in [a, b]$ and set $p = \gamma(t)$. Let U be a normal convex neighborhood of p (so $exp_p^{-1}: U \to T_pM$ is a diffeomorphism onto a star-shaped neighborhood of $0 \in T_pM$). For $q, r \in U$ distinct and such that the vectors $v_q = exp_p^{-1}(q),\ v_p = 0,\ v_r = exp_p^{-1}(r) \in T_pM$ are non-collinear, there exists a unique Euclidean circle $\widetilde{C} \subset T_pM$ through $v_q, 0, v_r$. Its image $C := exp_p(\widetilde{C}) \subset U$ is the exponential circle through q, p, r. When two arcs of C join q and r we select the minor arc (central angle $|\theta| < \pi$ measured in T_pM). The associated oriented sector is the image under exp_p of the corresponding Euclidean sector in T_pM, and its oriented area (computed with the induced Riemannian area form on that $2D$ surface) is denoted

$$A(p; q, r).$$

4.2. Compatibility (arc-multiplicity) assumption for partitions

For a partition $P = \{t_0 < t_1 < \ldots < t_N\}$ with mesh $\|P\| = h$, we require that each circular arc used in the sum is an integer multiple of a (chosen) reference minor arc length l_{min}. Concretely, for each segment *j* of the partition we require

$$l_j = m_j l_{min}, \qquad m_j \in N^+,$$

where l_j is the length of the minor arc associated to the triple $\left(\gamma(t_{j-1}), \gamma(t_j), \gamma(t_{j+1})\right)$. This guarantees angular/additive consistency across adjacent sectors and prevents orientation ambiguities in the limit.

Remark: The reference arc length l_{min} is defined locally with respect to the osculating (or exponential) circle at each point. Therefore, all multiples $m_j l_{min}$ share the same local radius R_j, ensuring consistency of the circular geometry within that segment. This construction guarantees that each curve possesses a well-defined intrinsic area, independent of any choice of secant axes, as formally established by the following convergence theorem.

4.3. Theorem: Convergence and determinacy of the minor-arc sector sum

Theorem: Under the standing assumptions above there exists $h_0 > 0$ such that for any partition $P = a = t_0 < \ldots < t_N = b$ with mesh $\| P\| = h < h_0$ the sector areas

$A_i := A\left(\gamma\left(t_i\right); \gamma\left(t_{i-1}\right), \gamma\left(t_{i+1}\right)\right), \qquad i = 1, \ldots, N-1$, are well defined and the sum

$S(P) = \sum_{i=1}^{N-1} A_i$ converges to a limit $S(\gamma)$ as $h \to 0$, independently of the choice of partitions with $\| P\| \to 0$. Moreover, for regular partitions one has the global error estimate $|S(P) - S(\gamma)| \leq C(b-a)\, h^2$, so $S(P) \to S(\gamma)$ with rate $O\left(h^2\right)$.

Proof of Theorem

The proof has four parts: (A) local reduction to a Euclidean tangent-plane problem and establishment of an $O\left(h^3\right)$ local bound; (B) summation over the partition to obtain an $O\left(h^2\right)$ global bound; (C) treatment of junctions/intersections to show left/right consistency and absence of jumps; (D) identification with Euclidean limit via charts.

a. Step A — Local expansion and $O\left(h^3\right)$ error per triplet

Fix i and consider the triple $\left(t_{i-1}, t_i, t_{i+1}\right)$ with $t_{i+1} - t_{i-1} \leq 2h$. Let $p = \gamma\left(t_i\right)$ and use normal coordinates centered at p. In these coordinates the exponential map admits the expansion

$$exp_p(w) = p + w + \frac{1}{2}\Gamma_p(w, w) + R_{exp}(w),$$

where $\Gamma_p(w, w)$ is quadratic in w (Christoffel terms) and $R_{exp}(w) = O\left(\| w\|^3\right)$ uniformly as $\| w\| \to 0$. Also put $\widetilde{\gamma} = exp_p^{-1} \circ \gamma$; since $\gamma \in C^3$,

$$\widetilde{\gamma}(s) = \widetilde{\gamma}(0) + \widetilde{\gamma}'(0)s + \frac{1}{2}\widetilde{\gamma}''(0)s^2 + R_\gamma(s), \qquad R_\gamma(s) = O\left(s^3\right).$$

Let $v' = \widetilde{\gamma}(-\delta)$, $v = 0$, $v'' = \widetilde{\gamma}(+\delta)$ with $\delta \leq h$. The unique Euclidean circle in T_pM passing through $v', 0, v''$ has radius $\widetilde{r}$ and central angle $\widetilde{\theta}$. Its sector area $\widetilde{A}$ approximates the sector area A obtained by first mapping the circle forward via exp_p. Because exp_p differs from the identity by terms $O\left(\| w\|^2\right)$ and the curve expansion has $O\left(h^3\right)$ remainder, a careful Taylor bookkeeping gives

$$\left|A - \widetilde{A}\right| \leq C_1 h^3$$

Moreover, classical planar 3-point circular interpolation estimates (osculating circle approximation) show that $\widetilde{A}$ approximates the true oriented area under γ over the small interval with an $O\left(h^3\right)$ difference as well. Combining yields the per-triplet local error

$$\left|A_i - A_i\right| \leq C_2 h^3,$$

where A_i denotes the exact oriented area contribution of γ on the corresponding tiny interval.

Detailed Taylor computations:

If $s \mapsto (s, y(s))$ is a planar representation of the curve in coordinates, expanding $y(s)$ about 0,

$$y(s) = y(0) + y'(0)s + \frac{1}{2}y''(0)s^2 + \frac{1}{6}y^{(3)}(0)s^3 + O(s^4).$$

Constructing the unique circle through $(-\delta, y(-\delta)), (0, y(0)), (\delta, y(\delta))$ and expressing its center and radius via determinants yields expansions for $\tilde{r}$ and $\tilde{\theta}$ that, after substitution into $\frac{1}{2}\tilde{r}^2\tilde{\theta}$, match the area under the cubic Taylor polynomial up to $O(h^3)$. The Riemannian corrections (via Γ_p and R_{exp}) only produce higher-order $O(h^3)$ differences because the exponential map is second-order accurate in normal coordinates.

b. Step B — Global summation and $O(h^2)$ rate

For a regular partition with mesh h we have $N = O(1/h)$. Summing the local bounds,

$$\sum_i |A_i - A_i| \leq \sum_i C_2 h^3 = C_2 N h^3 = C_2 (b - a) h^2.$$

Thus the family $\{S(P)\}$ is Cauchy as $h \to 0$, hence convergent; the limit is independent of the partition because the error depends only on the mesh, not on the particular nodes.

c. *Step C — Left/right consistency at circle intersections (Lemma)*

Consider a point $p = \gamma(t_*)$ that is the limit point of partition nodes from both sides. Suppose for one family of partitions the left sector is obtained from an exponential circle with parameters (R^L, θ^L) and the right sector from (R^R, θ^R). Working in normal coordinates we obtain expansions

$$R^L = R_0 + \alpha_L h + O(h^2), \quad \theta^L = \beta_L h + O(h^2),$$

$$R^R = R_0 + \alpha_R h + O(h^2), \quad \theta^R = \beta_R h + O(h^2),$$

where R_0 is the limiting osculating radius at p and $\beta_{L,R}$ are proportional to local geodesic curvatures. Since $\gamma \in C^3$, curvature and its one-sided limits coincide: $\beta_L = \beta_R$. Expanding sector areas,

$$A^L = \frac{1}{2}(R^L)^2 \theta^L = \frac{1}{2}R_0^2 \beta h + O(h^2), \qquad A^R = \frac{1}{2}R_0^2 \beta h + O(h^2),$$

hence $A^L - A^R = O(h^2)$. The same holds for arc lengths. This proves Lemma 5.1: no jump discontinuity occurs at junctions, and the sum is locally additive in the limit.

d. Step D — Identification with Euclidean limit

If γ is represented in a single Euclidean chart (or locally via normal coordinates), the above expansions show that the intrinsic exponential-sector construction reduces to the planar three-point circular sector construction up to $O\left(h^3\right)$ per triplet. Therefore, the global limit coincides with the Euclidean arc-based limit defined earlier. This completes the proof.

Lemma - Left/right consistency and asymptotic symmetry at circle intersections

Under the hypotheses of Theorem, for any partition family with mesh $h\to 0$, if two exponential circles used on the left and right of a meeting point p have parameters $\left(R_h^L, \theta_h^L\right)$, $\left(R_h^R, \theta_h^R\right)$, then

$$A_h^L - A_h^R = O\left(h^2\right),$$

and similarly

$$l_h^L - l_h^R = O\left(h^2\right).$$

This property was established in Step C of the main proof

4.4. Corollary 1 — Finite circular decomposition

Let $f: [a,b]\to R$ be C^2 with bounded curvature on $[a,b]$. Then there exists a finite partition $a = x_0 < \ldots < x_N = b$ and arcs γ_j (exponential or osculating circular arcs) such that $\gamma([a,b]) = \bigcup_{j=1}^{N} \gamma_j$, $l_j = m_j l_{min}$, $m_j \in N^+$, and the list $\{\left(R_j, \theta_j\right)\}_{j=1}^{N}$ describes all arcs composing γ.

Proof (sketch)

Since curvature $\kappa(s)$ is bounded on the compact interval, there exists a positive lower bound for the smallest local minor-arc length when choosing sufficiently small sample step. By the compatibility assumption we can choose l_{min} small enough so that every local osculating arc length is an integer multiple of l_{min} after a finite adaptive refinement; because $[a,b]$ is compact, only finitely many refinements are needed. The algorithm in §5.5 constructs such a partition (see algorithmic section).

Consequently, the set of exponential (or osculating) circles associated with the partition provides a continuous, curvature-matched covering of $\gamma([a,b]$, ensuring that the limit of the sector-area summation accounts for the entire curve.

5. Definition of the D'Ambrosio Integral

We now give the full definition, including the domain conditions and multiplicity constraint.

Let $f \in C^2([a,b])$. For a partition $P = \{x_0 < \ldots < x_n\}$ with mesh $\| P \|$, for each interior node x_i consider the consecutive triple $\left(x_{i-1}, x_i, x_{i+1}\right)$ and let the unique circle through the three points of the graph $\left(x_{i\pm1}, f\left(x_{i\pm1}\right)\right)$ have radius r_i and central angle θ_i. Denote the oriented sector area by

$$A_i = \frac{1}{2} r_i^2 \theta_i$$

(with sign according to orientation). Assume the partition satisfies the arc-multiplicity compatibility $l_i = m_i l_{min}$ for a chosen $l_{min} > 0$. Define the oriented D'Ambrosio sum

$$S(P) = \sum_{i=1}^{n-1} A_i.$$

Then define the D'Ambrosio integral (area) as

$$D[f] := \lim_{\|P\| \to 0} S(P),$$

provided the limit exists (Theorem guarantees existence for C^3 immersed graphs and in the Riemannian intrinsic formulation under the stated injectivity and curvature bounds).

The D'Ambrosio length functional is analogously

$$D_{length}[f] := \lim_{\|P\| \to 0} \sum_{i=1}^{n-1} r_i \left|\theta_i\right|.$$

Domain: the functional is defined on curves (or graph functions) for which all required exponential circles exist within a chosen normal neighborhood (injectivity radius condition) and where the arc-multiplicity condition can be enforced by refinement.

We define the total area functional as

$$A_{total}[f] := \lim_{max\left|x_{i+1} - x_i\right| \to 0} \sum_{i=1}^{n-1} \left(\frac{1}{2} r_i^2 \theta_i + r_i \left|y_i\right| \theta_i \right),$$

where r_i and θ_i are the radius and central angle of the osculating/exponential circle passing through the triple of points

$$\left(x_{i-1}, f\left(x_{i-1}\right)\right), \quad \left(x_i, f\left(x_i\right)\right), \quad \left(x_{i+1}, f\left(x_{i+1}\right)\right),$$

and y_i denotes the vertical coordinate of the circle center relative to the x-axis.

The first term, $\frac{1}{2} r_i^2 \theta_i$, represents the oriented sector area associated with the local curvature. The second term, $r_i \left|y_i\right| \theta_i$, approximates the area between the circular arc and the x-axis by projecting the sector's center onto the x-axis.

Taking the limit as the partition mesh goes to zero gives a functional $A_{total}[f]$ that combines the classical area under the curve with the curvature-induced sector areas, yielding a more precise geometric measure of the graph.

5.1. Properties of the D'Ambrosio Integral

We present the principal mathematical properties with their justifications.

- Linearity

For f, g in the domain and scalar α,

$$D[f + g] = D[f] + D[g], \qquad D[\alpha f] = \alpha D[f].$$

For a fixed partition, the oriented sector area of the vertical sum $f + g$ equals the sum of oriented sector areas of f and g up to higher-order terms; the $O\left(h^2\right)$ control preserves linearity in the limit.

- Additivity (locality)

For $a < c < b$,

$$D_{[a,b]}[f] = D_{[a,c]}[f] + D_{[c,b]}[f].$$

Choose partitions that include c; apply Lemma to avoid jump terms at c.

- Consistency with Riemann

If $f \in C^2([a, b])$, then

$$D[f] = \int_a^b f(x)\, dx.$$

Proof outline: The difference per triplet is $O\left(h^3\right)$; summing over $O(1/h)$ triplets gives $O\left(h^2\right)$ total difference, vanishing as $h \to 0$.

- Curvature sensitivity

The leading behavior of each sector depends on the curvature κ (via $r_i \approx 1/\kappa$); therefore, $D[f]$ encodes second-order geometric information, making it more accurate than first-order (straight segment) approximations in curved regions.

- Reparametrization invariance for length functional

The quantity $D_{length}[f]$ depends only on geometric arc lengths (sum of arc lengths), hence invariant under smooth monotone reparameterizations.

- Stability

Small C^2 perturbations of f produce small changes in $D[f]$. More precisely, if $\| f - g\|_{C^2} \leq \varepsilon$ then $|D[f] - D[g]| \leq C\varepsilon$ for small ε.

- Locality / domain dependence

The definition is local: all triples must lie in a common normal neighborhood to use exponential circles. Where curvature or injectivity radius conditions fail, the construction must be localized or replaced by a limiting procedure.

5.1.1. Convergence for smooth functions

Let $f: [a, b] \to R$ be a function of class C^2. For such functions, the existence of a unique osculating circle at each point guarantees that, over sufficiently small subintervals, the arc defined by three adjacent points of f provides a closer approximation to the function than a straight line segment. In the limit, as the partition norm $\|P\| \to 0$, the area under the interpolating circular arc converges to the area under the curve $f(x)$ over that subinterval.

$$\lim_{\|P\|\to 0} \sum_{i=0}^{n-2} A\left(\gamma_i\right) = \int_a^b f(x)\, dx$$

The Taylor expansion of $f(x)$ around $x = x_{i+1}$ demonstrates that the interpolating circle matches f to second order. The area under the arc differs from the area under f by a quantity of order $O\left(h^3\right)$, where $h = x_{i+2} - x_i$. Since the number of arcs is $O(1/h)$, the total error tends to zero as $h \to 0$. Hence, for sufficiently smooth functions, the D'Ambrosio Integral recovers the Riemann integral in the limit.

5.1.2. Geometric fidelity and curvature sensitivity

The D'Ambrosio Integral explicitly incorporates curvature into its formulation , offering a higher degree of geometric fidelity than standard linear approximation methods. When integrating over curves that exhibit sharp changes in concavity, or other types of pronounced curvature, the D'Ambrosio Integral provides a more accurate and faithful representation of the curve's geometry. This is particularly beneficial in scenarios where precise curvature analysis is crucial, such as in geometric modeling, physics simulations, or engineering applications involving structural integrity and material behavior.

This method proves to be especially advantageous when the function in question undergoes rapid local variations in curvature, as the D'Ambrosio Integral captures these variations with greater accuracy than methods that rely on piecewise linear approximations.

To illustrate the theoretical formulation of the D'Ambrosio Integral, we now present a worked example. By applying the method to a simple, well-understood function such as a parabola, we highlight the practical implementation of the new integral and the geometric precision it introduces.

Consider the function

$$f(x) = -x^2$$

on the interval $[-1, 1]$. This function is continuous and twice differentiable, with second derivative:

$$f''(x) = -2 < 0$$

The negative second derivative indicates that the function is concave, meaning its curvature bends downward. Furthermore, the function satisfies the conditions needed to apply the D'Ambrosio Integral.

For each triplet of consecutive points x_{i-1}, x_i, x_{i+1}, we consider the circle passing through the points $(x, f(x))$, and compute:

- The radius r_i
- The central angle θ_i

Using the D'Ambrosio Integral formulas, we approximate the area under the curve and the arc length as follows:

$$D[f] \approx \sum_{i=1}^{n-1} \frac{1}{2} r_i^2 \theta_i \quad \text{(Area approximation)}$$

$$D_{length}[f] \approx \sum_{i=1}^{n-1} r_i \theta_i \quad \text{(Arc length approximation)}$$

As $n \to \infty$, these expressions converge to the true area and length of the curve.

This geometric approach emphasizes local curvature and provides a more nuanced understanding of the curve compared to traditional methods.

The figure 1 shows the graphical representation of the D'Ambrosio Integral approximation applied to a concave parabola f(x)=−x2f(x) = -x^2f(x)=−x2.

Figure 1 – Graphical representation of D'Ambrosio Integral approximation (Concave Parabola)

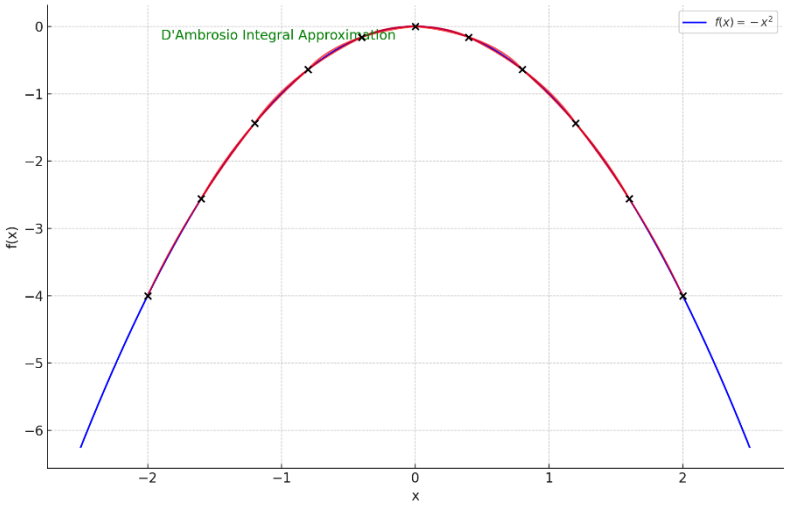

- The blue curve is the true function.
- The red arcs represent the circular sectors used in the D'Ambrosio method, highlighting the curvature-based approximation.
- The black dots are the sample points used to construct each triplet that defines the arcs.

This visualization showcases how the D'Ambrosio approach captures the curved nature of the graph more faithfully than traditional linear approximations like in Riemann sums.

5.2 Extensions and generalizations of the D'Ambrosio Integral

In this section, we outline several theoretical extensions of the D'Ambrosio Integral beyond its initial formulation for real-valued functions of one variable. We discuss its applicability to parametric curves, vector-valued functions, and its potential for generalization to higher-dimensional domains.

5.2.1 Parametric curves in $\mathbb{R}^2$

Let $\gamma: [a, b] \to R^2$ be a twice-differentiable curve, $\gamma(t) = (x(t), y(t))$, with $t \in [a, b]$. For such curves, we define the D'Ambrosio integral as a summation over arcs of circles interpolating three consecutive points $\gamma(t_i)$, $\gamma(t_{i+1})$, and $\gamma(t_{i+2})$, where $t_0, t_1, \ldots, t_n$ is a partition of $[a, b]$.

The D'Ambrosio arc integral of γ over $[a, b]$ is given by:

$$\int_a^b d \circ \gamma := \lim_{\|P\| \to 0} \sum_{i=0}^{n-2} A\left(C_i\right),$$

where $A\left(C_i\right)$ denotes the signed area under the circular arc connecting $\gamma\left(t_i\right)$, $\gamma\left(t_{i+1}\right)$, and $\gamma\left(t_{i+2}\right)$, oriented consistently with the curve's parametrization.

This construction preserves geometric meaning in the plane and accounts for local curvature changes. It is particularly useful in applications involving motion along a path, shape reconstruction, and contour analysis.

5.2.2. Potential extension to complex functions

The geometric foundation of the D'Ambrosio Integral naturally extends to the complex plane. Given that any three distinct non-collinear points in $\mathbb{C}$ determine a unique circumcircle, an arc-based integral may be defined along complex curves, particularly for analytic functions defined on smooth contours.

This approach may yield a novel geometric interpretation of complex integration. While the classical Cauchy Integral relies on pointwise evaluations and infinitesimal paths, the D'Ambrosio-type complex integral incorporates local curvature information, potentially enriching the understanding of conformal mappings and holomorphic flow. For instance, the integral of a complex-valued function f: $\mathbb{C} \to \mathbb{C}$ over a Jordan curve γ might be approximated by summing the oriented contributions of circular arcs connecting consecutive triplets of points sampled along γ.

Additionally, such an integral could be relevant in the context of discrete complex analysis, where circle packings and curvature-sensitive approximations are used to discretize conformal structures (Stephenson, 2005). This could open pathways to reinterpret classical theorems—such as Cauchy's or the residue theorem—via curvature-aware formulations, especially in numerical conformal geometry and geometric function theory.

The following corollaries illustrate how the theoretical framework of the D'Ambrosio Integral extends naturally to the setting of differential fields and parameter-dependent dynamical systems on manifolds

5.3. Corollary 2 — Application to differential fields

Let $X \in C^1(M, TM)$ be a smooth vector field on (M, g) generating a local flow Φ_t. For $\xi \in M$ set $\gamma_\xi(t) = \Phi_t(\xi)$ and suppose $\gamma_\xi([0, T])$ lies within a tubular normal neighborhood with injectivity radius $r_{min} > 0$ and that $\gamma_\xi \in C^3$.

Then the Theorem applies to γ_ξ and the oriented sector sum along γ_ξ converges to $S\left(\gamma_\xi\right)$.

Define $S_X(\xi) := S\left(\gamma_\xi\right)$. Standard results on smooth dependence of ODE solutions on initial data imply S_X is C^1 (indeed smooth) on the open set of initial conditions whose flow remains inside the chosen normal neighborhood.

Hence S_X is a curvature-sensitive integral invariant associated with the flow of X. This invariant can be used in applications to distinguish flow lines by their accumulated geometric sweep.

This provides a powerful tool for analyzing how the global geometric behavior of trajectories changes with the variation of parameters in a dynamical system defined on a curved space.

Remark.
The earlier formulation for vector-valued functions $f: [a, b] \to Rn$, expressed in terms of the surface area swept by interpolating arcs, appears as a particular instance of the present construction. Indeed, the flow lines of a smooth vector field $X \in C^1(M, TM)$ can be regarded as vector-valued curves $\gamma\xi(t)$, and the curvature-sensitive invariant S_X extends this geometric principle to Riemannian manifolds, preserving the same curvature-aware integration structure.

5.4. Corollary 3 — Families and bundles of differential equations

Let $X: M \times \Lambda \to TM$ be C^1 in both variables and smoothly dependent on parameters $\lambda \in \Lambda \subset R^k$. Under uniform injectivity-radius and curvature bounds on the parameter family, the Theorem applies uniformly and the functional $S_{X_\lambda}(\xi) = S\left(\gamma_{\xi,\lambda}\right)$ depends smoothly on (ξ, λ).

Consequently $\lambda \mapsto S_{X_\lambda}(\xi)$ is a smooth map and the family $\{S_{X_\lambda}\}_{\lambda \in \Lambda}$ forms a smooth bundle of curvature-sensitive invariants.

5.5. Explicit formulas for circles: the Algorithm to obtain finite arc decomposition

To implement the construction numerically (or to give explicit formulas for the arcs composing a planar graph), one needs closed expressions for the circumcenter, radius, central angle and area. Given three non-collinear points $P_1 = \left(x_1, y_1\right)$, $P_2 = \left(x_2, y_2\right)$, $P_3 = \left(x_3, y_3\right)$ in R^2, define the determinant

$$D = 2|x_1\ y_1\ 1\ x_2\ y_2\ 1\ x_3\ y_3\ 1\ |.$$

Set

$$U = |x_1^2 + y_1^2\ y_1\ 1\ x_2^2 + y_2^2\ y_2\ 1\ x_3^2 + y_3^2\ y_3\ 1\ |, \qquad V = |x_1\ x_1^2 + y_1^2\ 1\ x_2\ x_2^2 + y_2^2\ 1\ x_3\ x_3^2 + y_3^2\ 1\ |.$$

Then the circumcenter $O = (u, v)$ is

$$u = \frac{U}{D}, \qquad v = -\frac{V}{D},$$

and the radius is

$$R = \sqrt{\left(x_1 - u\right)^2 + \left(y_1 - v\right)^2}.$$

The chord length between P_1 and P_3 is $c = \|P_1 - P_3\|$. The central angle $\theta \in (-\pi, \pi]$ of the minor arc satisfies

$$\theta = 2arcsin\left(\frac{c}{2R}\right),$$

with orientation determined by $atan2$ on vectors $\vec{a} = P_1 - O$, $\vec{b} = P_3 - O$:

$$\theta = atan2\left(det\left(\vec{a}, \vec{b}\right),\ \vec{a} \cdot \vec{b}\right).$$

Sector area and arc length are

$$A_{sector} = \frac{1}{2}R^2\theta, \qquad l = R|\theta|.$$

Degenerate / nearly collinear cases: If $|D|$ is numerically tiny, treat the triple as nearly collinear: use the oriented triangular area or refine the partition to avoid instability.

The numerical algorithm for obtaining the compatible arc decomposition—previously expressed as pseudocode—is now implemented and detailed in Appendix A, which provides the corresponding Python implementation.

5.6. Validity in non-Euclidean geometries

The construction is intrinsic because it uses the exponential map at each basepoint p and constructs circles in the tangent plane T_pM — these are then mapped back into M. Hence:

- Local existence: If three points q, r, s lie in a normal convex neighborhood of p of radius less than the injectivity radius, the exponential circle through $exp_p^{-1}(q), 0, exp_p^{-1}(r)$ exists and its image is a well defined 1-dimensional submanifold of that neighborhood. The minor arc selection uses the central angle computed in the tangent plane.
- Spherical geometry: On S^2 (or constant positive curvature manifolds) the exponential circles correspond to intersections of S^2 with (affine) planes — i.e., (great or small) circles. Three non-collinear points lying on a sufficiently small hemisphere always determine a unique circle (with the caveat of antipodal ambiguities if points are spread globally).
- Hyperbolic geometry: In hyperbolic models the tangent-plane construction produces geodesic circles or equidistant curves; centers may lie at infinity for limiting cases, so one must ensure triples remain in a bounded region where the tangent-plane reduction is valid.
- General Riemannian manifolds: Curvature appears in the expansions (via curvature tensor terms) and contributes only higher-order corrections (controlled by bounds on curvature and covariant derivatives). Therefore, the same $O\left(h^3\right)$ local estimates hold locally and Theorem 2 extends provided triples are inside normal neighborhoods and curvature/injectivity bounds are uniform along γ.

Therefore, the D'Ambrosio Integral is intrinsically local and transfers to non-Euclidean settings via exponential circles, with the same convergence and determinacy properties under the stated geometric assumptions.

5.7. Final discrete representation formula and concluding remarks

Combining the previous results we may assert that, for any C^2 curve γ with bounded curvature on a compact interval, there exists a finite decomposition into exponential/osculating circular arcs satisfying the multiplicity condition, and the D'Ambrosio integral is computed as the limit of the oriented sum of sector areas:

$$S(\gamma) = \lim_{\|P\|\to 0} \sum_{i=1}^{N-1} \frac{1}{2} r_i^2 \theta_i$$

and, for the finite decomposition produced by the algorithm,

$$\gamma(t) = \bigcup_{j=1}^{N} \gamma_j(t), \qquad S(\gamma) \approx \sum_{j=1}^{N} \frac{1}{2} R_j^2 \Theta_j,$$

with

$$l_j = R_j\left|\Theta_j\right| = m_j l_{min}, \qquad m_j \in N^+.$$

This discrete formulation provides a constructive representation of the curve as a finite concatenation of curvature-consistent arcs.
The resulting integral preserves the classical Riemann value for smooth functions while ensuring second-order geometric accuracy in regions of significant curvature and extending naturally to Riemannian manifolds.

6. Theoretical and practical implications

The D'Ambrosio Integral introduces a novel approach to integration by replacing linear segments used in classical Riemann sums with arcs of circles determined by consecutive non-collinear point triplets. While the Riemann integral and its Lebesgue and Henstock–Kurzweil generalizations focus on partitioning the domain of integration and summing function values against linear measures (Bartle, 1996; Gordon, 1994), the D'Ambrosio Integral introduces a second-order geometric primitive—the circular arc—as the basic unit of approximation. This transition from linearity to curvature-sensitive interpolation represents a departure from standard integral theory.

This formulation is not merely a geometric reinterpretation but a distinct mathematical object with its own implications. While some studies have explored geometric quadrature based on curvature corrections or adaptive meshes (Farouki & Neff, 1990; Mäkinen, 1993), none, to our knowledge, have proposed a summation framework where arcs of circumcircles are the fundamental approximation units. Unlike spline-based integrators or Gaussian quadrature methods tailored to specific weight functions (Davis & Rabinowitz, 1984), the D'Ambrosio Integral builds curvature directly into the construction of the partition elements, without requiring additional function evaluations or derivative estimates.

Moreover, the integral is defined not merely by the curvature of the function graph, but by the geometric relationships among point samples—aligning it with recent interest in discrete differential geometry and data-driven approximation (Crane et al., 2013). This opens up new paths for integrating functions that are represented discretely, as in shape analysis, computational anatomy, or machine learning tasks involving structured geometric data.

The D'Ambrosio Integral presents several promising implications for numerical integration and approximation theory, both from theoretical and computational standpoints.

From a theoretical perspective, the arc-based summation scheme suggests a new family of integral approximations that bridge classical Riemann integration and geometric modeling. By embedding local curvature directly into the integration process, the D'Ambrosio Integral may improve convergence behavior for functions with high geometric complexity. Unlike standard Riemann sums, which suffer from poor approximation near inflection points or rapidly changing gradients, arc-based sums can better conform to the local geometry of the integrand (Fletcher, 2001).

This has direct consequences for approximation theory. The D'Ambrosio approach may inspire a new class of quadrature rules—what might be called "geometric quadratures"—in which partition elements are selected not merely based on arc length or uniform spacing, but on local curvature metrics. This would represent a refinement over existing adaptive quadrature schemes that only adjust interval widths (Piessens et al., 1983). Furthermore, circular interpolants naturally preserve higher-order continuity and could thus provide superior approximations in contexts where second derivatives are meaningful.

Beyond the planar setting, the integral admits an intrinsic Riemannian formulation via exponential circles. In particular, the construction yields a smooth invariant $S_X(\xi)$ when applied to integral curves of a C^1 vector field X (Corollary 2), and a parameter-dependent family of such invariants when the vector field depends on parameters (Corollary 3). These results show that the

D’Ambrosio Integral is both a local curvature-sensitive quadrature and a global, curvature-aware descriptor of flow geometry on manifolds.

Practically, this could be transformative in domains such as computer graphics, geometric modeling, and physical simulations, where object boundaries and motion trajectories are inherently curved. In spline fitting and mesh generation, for example, using arc-based integrals may yield smoother, more physically faithful approximations. The method may also benefit simulations in mechanics or fluid dynamics, where geometric fidelity of boundary integrals affects stability and accuracy (Batty & Bridson, 2008).

Moreover, the discrete construction of the D’Ambrosio Integral aligns with more recent trends in data-driven numerical methods and discrete differential geometry, particularly in situations where only point samples of a function or shape are available (e.g., Sifakis et al., 2019; Zhang et al., 2021). In such cases, reconstructing a curvature-sensitive integral from sparse data could offer significant advantages over classical methods, which typically rely on dense sampling or smoothness assumptions for the underlying function (Wang & Brugiapaglia, 2022). This approach opens up new possibilities for geometric analysis in applications like machine learning, computational geometry, and the analysis of irregular, high-dimensional data.

From a computational standpoint, for example, the finite-arc decomposition algorithm (Appendix A) provides a constructive procedure to obtain partitions satisfying the multiplicity condition. This makes the method directly implementable for curvature-preserving quadrature and enables stable discretizations of curved trajectories on both Euclidean domains and within normal neighborhoods on Riemannian manifolds.

7. Conclusions, limitations, and future research

This paper introduced the D’Ambrosio Integral, a novel curvature-sensitive reformulation of the Riemann integral in which summation is performed over arcs of circles interpolating triplets of points. The construction preserves key properties of integration while introducing a new geometric layer particularly suited for applications involving curved shapes, motion, and digital reconstruction.

By extending the classical linear approximation of Riemann sums to a second-order geometric interpolant, the D’Ambrosio Integral offers both theoretical and practical advantages in fields where local curvature plays a critical role. We have outlined its formal definition, its equivalence to Riemann's integral in the limit, and its adaptability to parametric curves and complex-valued functions. Possible generalizations to higher-dimensional surfaces and function spaces were also explored.

Nevertheless, several limitations and open questions remain. The current formulation assumes sufficient regularity—at least C^2 continuity—to ensure the uniqueness of interpolating circular arcs. For more general function classes, such as those in L^2 or bounded variation (BV), the absence of differentiability may hinder the well-posedness of arc construction. Future work could explore the use of geometric surrogates, such as least-squares circle fits or curvature-averaged arc approximations, to extend the integral to broader functional spaces.

Additionally, the increased computational complexity of determining and evaluating circular arcs, compared to linear segments, poses a trade-off between geometric fidelity and numerical efficiency. Analytical tools for estimating error bounds, convergence rates, and stability under partition refinement remain to be developed.

We believe that the D’Ambrosio Integral opens up promising directions for numerical analysis, differential geometry, and applied mathematics. In particular, its geometric foundation makes it well-suited for incorporation into shape-aware numerical methods, curvature-adaptive integration schemes, and possibly into discretized versions of complex and harmonic analysis.

Importantly, the corollaries extend the D’Ambrosio Integral from a planar quadrature to a family of curvature-sensitive invariants for dynamical systems on manifolds. The intrinsic formulation via the exponential map ensures coordinate independence, while the accompanying algorithm

establishes practical feasibility. These combined theoretical and computational aspects suggest immediate opportunities for structure-preserving numerical methods and for geometric analysis of flows on curved spaces.

Future research on the D'Ambrosio Integral holds great potential for expanding its applicability across a variety of mathematical and computational domains. Some key directions for further exploration include:

1. Extensions to noisy or stochastic settings. The current formulation of the D'Ambrosio Integral assumes relatively smooth and well-behaved functions, but many real-world datasets are noisy or exhibit stochastic behavior. Extending the integral to such settings could expand its applicability in fields like signal processing, data science, and machine learning. One promising direction involves integrating noise-robust techniques while preserving sensitivity to curvature. For instance, total variation regularization has proven effective in denoising while maintaining structural features (Rudin et al., 1992). Recent advancements in curvature-preserving denoising have introduced high-order variational models that incorporate curvature-based regularization, effectively preserving geometric features in images and surfaces. For instance, a novel image denoising approach utilizes the sum of squared principal curvatures of the image surface to enhance detail preservation and reduce staircase artifacts (Chankan et al., 2023) In the realm of stochastic differential equations (SDEs), significant progress has been made in developing numerical methods that preserve the underlying geometric structures. Structure-preserving stochastic Runge–Kutta–Nyström methods have been proposed for nonlinear second-order SDEs with multiplicative noise, ensuring the conservation of quadratic invariants and symplectic structures over long-time simulations (Ma et al., 2019). Furthermore, recent studies have focused on stochastic multisymplectic partial differential equations (PDEs), constructing stochastic multisymplectic systems and developing structure-preserving collocation methods that maintain discrete analogues of stochastic conservation laws (Hu & Peng, 2025). These advancements in curvature-preserving denoising and structure-preserving numerical methods for SDEs and PDEs provide promising directions for extending the D'Ambrosio Integral to handle noisy or stochastic settings while maintaining its curvature-sensitive nature.
2. Applications in computer vision and 3D surface reconstruction. Given its curvature-sensitive design, the D'Ambrosio Integral is well-suited for computer vision tasks like 3D surface reconstruction, mesh refinement, and shape analysis. These applications often deal with incomplete, sparse, or noisy point clouds. Integrating a curvature-aware integral could improve geometric accuracy in surface fitting, especially around sharp features or discontinuities. Recent advances in deep learning-based surface reconstruction emphasize the importance of capturing local curvature for accurate 3D modeling (Erler et al., 2020).
3. Riemannian manifolds, differential fields, and computational generalizations. The D'Ambrosio Integral has been formally extended to Riemannian manifolds through curvature-sensitive invariants, providing an intrinsic, coordinate-independent formulation. Future research could focus on both theoretical and computational aspects in this context. On the theoretical side, the curvature-sensitive invariants, such as $S_X(\xi)$, offer new tools for analyzing trajectories of dynamical systems on manifolds, with potential applications in stability and bifurcation studies of nonlinear flows. On the computational side, further work is needed to optimize the algorithmic construction of curvature-compatible partitions, implement adaptive mesh refinement, and develop efficient numerical schemes for high-dimensional manifolds. These advances could enable practical applications in geometric computing, manifold-based machine learning, and large-scale data analysis, while preserving the curvature-aware properties of the integral.
4. Connections with fractional calculus and non-local operators. Fractional calculus offers powerful tools for modeling non-local and memory-dependent phenomena, which often arise in biological systems, materials science, and finance. These non-local behaviors parallel the

curvature-based generalization proposed in the D'Ambrosio Integral. Exploring how curvature-aware integration might intersect with fractional operators could lead to novel hybrid models capable of capturing both geometric and long-range interactions. Recent developments in fractional modeling point to growing interest in this direction (Meerschaert & Sikorskii, 2019).

These research directions highlight the broad and multidisciplinary impact that the D'Ambrosio Integral could have on both theoretical mathematics and applied fields. By addressing these challenges, future work could significantly extend the utility of the integral, fostering deeper insights into both mathematical theory and practical applications.

References

Bartle, R. G. (1996). A Modern Theory of Integration. American Mathematical Society.

Bartle, R. G. (2014). *The elements of integration and Lebesgue measure*. John Wiley & Sons.

Batty, C., & Bridson, R. (2008). Accurate viscous free surfaces for buckling and collapse. ACM Transactions on Graphics, 27(3), 100.

Botsch, M., Kobbelt, L., Pauly, M., Alliez, P., & Lévy, B. (2010). *Polygon mesh processing*. CRC press.

Bronstein, M. M., Bruna, J., Cohen, T., & Veličković, P. (2021). Geometric deep learning: Grids, groups, graphs, geodesics, and gauges. *arXiv preprint arXiv:2104.13478*.

Chami, I., Ying, Z., Ré, C., & Leskovec, J. (2019). Hyperbolic graph convolutional neural networks. *Advances in neural information processing systems*, *32*.

Chankan, S., Chumchob, N., & Sroisangwan, P. (2023). A novel image denoising approach based on a curvature-based regularization. *Signal, Image and Video Processing*, *17*(5), 2129-2136.

Chen, Q., Montesinos, P., Sun, Q. S., Heng, P. A., & Xia, D. S. (2010). Adaptive total variation denoising based on difference curvature. *Image and vision computing*, *28*(3), 298-306.

Crane, K., Weischedel, C., & Wardetzky, M. (2013). Geodesics in heat: A new approach to computing distance based on heat flow. ACM Transactions on Graphics (TOG), 32(5), 152.

Davis, P. J., & Rabinowitz, P. (1984). Methods of Numerical Integration. Academic Press.

do Carmo, M. P. (1992). *Riemannian Geometry*. Birkhäuser.

do Carmo, M. P. (2016). *Differential geometry of curves and surfaces: revised and updated second edition*. Courier Dover Publications.

Erler, P., Guerrero, P., Ohrhallinger, S., Mitra, N. J., & Wimmer, M. (2020, August). Points2surf learning implicit surfaces from point clouds. In *European Conference on Computer Vision* (pp. 108-124). Cham: Springer International Publishing.

Farouki, R. T., & Neff, C. A. (1990). Hermite interpolation and subdivision schemes for curves with rational offset. Computer Aided Geometric Design, 7(1–4), 101–115.

Fletcher, C. A. J. (2001). Computational Techniques for Fluid Dynamics. Springer.

Gordon, R. A. (1994). The Integrals of Lebesgue, Denjoy, Perron, and Henstock. American Mathematical Society.

Hairer, E., Hochbruck, M., Iserles, A., & Lubich, C. (2006). Geometric numerical integration. *Oberwolfach Reports*, *3*(1), 805-882.

Henstock, R. (1955). Definitions of Riemann type of the variational integral. *Proceedings of the London Mathematical Society*, 3(1), 402–418.

Hu, R., & Peng, L. (2025). Stochastic multisymplectic PDEs and their structure-preserving numerical methods. *arXiv preprint arXiv:2501.16913*.

Kloeden, P. E., & Platen, E. (1992). *Numerical Solution of Stochastic Differential Equations*. Springer.

Ma, Q., Song, Y., Xiao, W., Qin, W., & Ding, X. (2019). Structure-preserving stochastic Runge–Kutta–Nyström methods for nonlinear second-order stochastic differential equations with multiplicative noise. *Advances in Difference Equations*, *2019*, 1-18.

Mäkinen, J. (1993). Integration methods based on spline approximation. BIT Numerical Mathematics, 33(1), 32–44.

McShane, E. J. (1953). A Riemann-type integral that includes Lebesgue-Stieltjes, Bochner and stochastic integrals. *Memoirs of the American Mathematical Society*, 34.

Meerschaert, M. M., & Sikorskii, A. (2019). *Stochastic models for fractional calculus* (Vol. 43). Walter de Gruyter GmbH & Co KG.

Piessens, R., de Doncker-Kapenga, E., Überhuber, C. W., & Kahaner, D. K. (1983). Quadpack: A Subroutine Package for Automatic Integration. Springer.

Press, W. H., Teukolsky, S. A., Vetterling, W. T., & Flannery, B. P. (2007). *Numerical Recipes: The Art of Scientific Computing*, 3rd Edition. Cambridge University Press.

Riemann, B. (1867). *Ueber die Darstellbarkeit einer Function durch eine trigonometrische Reihe*. Dieterichschen Buchhandlung.

Royden, H. L. (1988). *Real Analysis*, 3rd Edition, Macmillan.

Rudin, L. I., Osher, S., & Fatemi, E. (1992). Nonlinear total variation based noise removal algorithms. *Physica D: nonlinear phenomena*, 60(1-4), 259-268.

Rudin, W. (1976). *Principles of Mathematical Analysis*, 3rd Edition, McGraw-Hill, Inc., USA.

Sifakis, E., Rusinkiewicz, S., & Durand, F. (2019). Curvature-aware data-driven analysis. *ACM Transactions on Graphics* (TOG), 38(2), 1-13.

Stephenson, K. (2005). Introduction to Circle Packing: The Theory of Discrete Analytic Functions. Cambridge University Press.

Wang, W., & Brugiapaglia, S. (2024). Compressive Fourier collocation methods for high-dimensional diffusion equations with periodic boundary conditions. IMA Journal of Numerical Analysis, 44(6), 3780-3814.

Zhang, X., Zhu, J., & Sun, Y. (2021). Geometry processing for irregular data. *Journal of Computational Physics*, 429, 109946.